(122)

GENERATION OF MODES FOR LOADED VEHICLE FROM EMPTY VEHICLE, DSV-IVB

APRIL 1964
DOUGLAS REPORT SM-46647

FACILITY FORM 602
N70-75887
(ACCESSION NUMBER)
(THRU)
NONE
(CODE)
24
(PAGES)
CR-113261
(NASA CR OR TMX OR AD NUMBER)
(CATEGORY)

GENERATION OF MODES FOR LOADED VEHICLE FROM EMPTY VEHICLE, DSV-IVB

APRIL 1964
DOUGLAS REPORT SM-46647

PREPARED BY: D.T. SHOHO
FLIGHT DYNAMICS AND CONTROL SECTION
SATURN ENGINEERING

PREPARED FOR:
NATIONAL AERONAUTICS
AND SPACE ADMINISTRATION
UNDER NASA CONTRACT NAS7-101

R E Holmen

APPROVED BY: R.E. HOLMEN
CHIEF, FLIGHT DYNAMICS AND CONTROL SECTION
SATURN ENGINEERING

T E Abraham

APPROVED BY: T.E. ABRAHAM
MANAGER, S-IVB SYSTEMS DEVELOPMENT

DOUGLAS MISSILE & SPACE SYSTEMS DIVISION

ABSTRACT

This technical report was prepared for presentation at the Vehicle Dynamics and Control Working Group meeting held at Douglas Aircraft Company's Huntington Beach Facility on February 25 - 27, 1964. The analysis was performed in compliance with the request made at the September 19, 1963, splinter meeting of the S-IVB Dynamics and Control Working Group, held at the Marshall Space Flight Center.

The report is transmitted to partially fulfill the requirements of Contract Number NAS7-101 as noted in Douglas Aircraft Company Report SM-41410, Data Submittal Document, Saturn S-IVB System, Item 3.8, dated March 1962.

TABLE OF CONTENTS

PARAGRAPH	TITLE	PAGE
	ABSTRACT	i
	TABLE OF CONTENTS	ii
	LIST OF ILLUSTRATIONS	iii
	LIST OF SYMBOLS	iv
	PREFACE	v
1.	INTRODUCTION	1
2.	ANALYSIS	3
2.1	100% Burn Time Characteristics	3
2.2	0% Burn Time Vehicle Inertial Characteristics	3
2.3	Transformation to Modal Coordinates	4
2.4	100% Burn Time Vehicle Elastic Characteristics	4
2.5	Equations of Motion	5
2.6	Solution of Equations for Frequencies and Mode Shapes	6
2.7	Generation of Modal Mass Matrix	6
3.	RESULTS	8
4.	CONCLUSIONS	10
	APPENDIX	14

LIST OF ILLUSTRATIONS

Figure	Description	Page
1.	First Mode Body Bending Deflection	11
2.	Second Mode Body Bending Deflection	12
3.	Third Mode Body Bending Deflection	13

List of Symbols

h_{1-32}	Translational Deflection of Stations 1 through 32 (inches)
h	Translational Deflection of Rigid Body Mode (inches)
α_{1-32}	Rotational Deflection of Stations 1 through 32 (radians)
θ	Rotational Deflection of Rigid Body Mode (radians)
T_{100}	Transformation Matrix Relating Sectional Deflections to 100% Burn Time Mode Shapes
T	Transformation Matrix Relating Sectional Deflections to 0% Burn Time Mode Shapes
$T_{100,0}$	Transformation Matrix Relating 100% Burn Time Modes to 0% Burn Time Modes
$\xi_{i,100}$	Generalized coordinate of ith mode at 100% Burn Time
$\xi_{i,0}$	Generalized coordinate of ith mode at 0% Burn Time
P_{1-32}	Force Applied at Station Numbers 1 through 32 (pounds)
$P_{\xi_{i,100}}$	Modal Forces at 100% Burn Time of ith mode (pounds)
P_h	Modal Force for the Rigid Body Translational Mode (pounds)
Q_θ	Moment for the Rigid Body Rotational Mode (inch pounds)
Q_{1-32}	Moments Applied from Station Numbers 1 through 32 (inch pounds)
M_0	Sectional Mass Matrix at 0% Burn Time
$\bar{M}_0$	Modal Mass Matrix at 0% Burn Time
$M_{i,100}$	Modal Mass of ith Mode at 100% Burn Time
M_1	Mass of the Vehicle (lb sec^2/inch)
I_{CG}	Moment of Inertia of the Vehicle (lb sec^2 inch)
$\bar{K}_{100}$	Spring Matrix at 100% Burn Time
$\omega_{i,100}$	Frequency of ith Mode at 100% Burn Time (Radians/sec)

NOTES

1. Double dots above any symbol denotes second derivative with respect to time.
2. Superscript "*" denotes transpose of matrix.
3. Superscript "'" denotes normalized matrix.

PREFACE

A study was performed to demonstrate the validity of determining the modal properties of the Saturn IB/S-IVB dynamics vehicle for any propellant loading given only a set of empty vehicle modes. The empty (100% burn time) modes were calculated by the Myklestad beam vibration method. Matrix algebra was employed to add the full propellant load (0% burn time) to the 100% burn time elastic and rigid body modes. The uncoupled gross vehicle modes were then calculated. This method of obtaining data produced a reasonable amount of accuracy in the first two modes. The accuracy of the third mode was poor and of limited value.

1. INTRODUCTION

The dynamic characteristics of the S-IVB Stage have to be determined for inclusion into the control system analysis. The dynamic characteristics can be determined empirically by the Dynamics Vehicle vibration tests. If a loaded (propellants on board) simulation is desired, substitute fluids must be used in place of hydrogen and oxygen. The Dynamics Vehicle cannot accept cryogenics. Any substituted liquid for hydrogen will have to compromise on density. Oxygen offers similar restrictions but it is possible to simulate LOX density, though with some difficulty. Furthermore, under the test conditions, there will always be a 1.0 g acceleration. Under the flight conditions, axial acceleration is different from 1.0 g the majority of the time. The acceleration discrepancy will cause the test sloshing frequency to be different than flight conditions. Thus, the actual simulation is achieved only when the vehicle is empty.

One way out of this dilemma is to measure only the empty modes on the Dynamics Vehicle. By matrix algebra methods, propellants can be added to the empty modes to obtain modes for any desired burn time.

The basis for this transformation lies in the fact that the vehicle's stiffness characteristics do not change for different propellant loadings. Addition of propellants to the empty modes alters the mass matrix by adding terms both to the diagonal and off diagonal terms. However, since the vehicle stiffness distribution does not change, the spring matrix will not change either. Thus the spring matrix and coupled mass matrix can be combined to form the equations of motion for the vehicle with propellants. These equations can then be solved to produce the frequencies and mode shapes for the loaded vehicle. The resulting mode shapes can then be used to generate the new (orthogonal) modal mass characteristics.

The above approach was demonstrated in this report for the Saturn IB/S-IVB Dynamics Vehicle. A set of 100% burn time (empty) modes were transformed to 0% burn time (fully loaded) modes.

2. ANALYSIS

2.1 100% Burn Time Characteristics

The input data calculated by the Myklestad beam vibration program includes the frequencies, the modal springs, and the mode shapes. The first three frequencies of the elastic modes were 6.7951, 20.946, and 45.581 cps. The modal masses were 88.56, 44.48, and 56.72 lb sec ^{2}/in for the first three modes respectively. The mode shapes at 100% burn time are contained in Appendix A-1. These mode shapes are repeated below in abbreviated form.

$$\begin{Bmatrix} h_1 \\ \alpha_1 \\ \vdots \\ h_{32} \\ \alpha_{32} \end{Bmatrix} = \begin{bmatrix} & & \\ & T_{100} & \\ & & \end{bmatrix} \begin{Bmatrix} \xi_{1,100} \\ \xi_{2,100} \\ \xi_{3,100} \\ h \\ \theta \end{Bmatrix} \tag{1}$$

Thus, the transformation matrix, T_{100}, describes the deflection of the vehicle sections, h_{1-32} and α_{1-32}, in terms of the first three bending modes and rigid body modes for 100% burn time.

2.2 0% Burn Time Vehicle Inertial Characteristics

The sectional mass characteristic at 0% burn time can be shown in matrix form.

$$\begin{Bmatrix} P_1 \\ M_1 \\ \vdots \\ P_{32} \\ M_{32} \end{Bmatrix} = \begin{bmatrix} & & \\ & M_0 & \\ & & \end{bmatrix} \begin{Bmatrix} \ddot{h}_1 \\ \ddot{\alpha}_1 \\ \vdots \\ \ddot{h}_{32} \\ \ddot{\alpha}_{32} \end{Bmatrix} \tag{2}$$

2.3 Transformation to Modal Coordinates

The modal masses are calculated by use of the 0% burn time sectional mass matrix and the 100% burn time transformation matrix. The sectional forces and sectional accelerations at 0% burn time were transformed into the modal forces and modal accelerations at 100% burn time by the operations of equation 3.

$$\begin{Bmatrix} P_{\xi_{1,100}} \\ P_{\xi_{2,100}} \\ P_{\xi_{3,100}} \\ P_h \\ Q_\theta \end{Bmatrix} = \begin{bmatrix} T_{100} \end{bmatrix}^* \begin{bmatrix} M_0 \end{bmatrix} \begin{bmatrix} T_{100} \end{bmatrix} \begin{Bmatrix} \ddot{\xi}_{1,100} \\ \ddot{\xi}_{2,100} \\ \ddot{\xi}_{3,100} \\ \ddot{h} \\ \ddot{\theta} \end{Bmatrix} \tag{3}$$

The manipulation, $\left[T_{100}\right]^*\left[M_o\right]\left[T_{100}\right]$, represents the integrated mass matrix, $\left[\bar{M}_o\right]$, of the 0% burn time vehicle in term of the 100% burn time forces and coordinates.

$$\begin{bmatrix} \bar{M}_0 \end{bmatrix} = \begin{bmatrix} T_{100} \end{bmatrix}^* \begin{bmatrix} M_0 \end{bmatrix} \begin{bmatrix} T_{100} \end{bmatrix} \tag{4}$$

2.4 100% Burn Time Vehicle Elastic Characteristics

The equations of the spring forces at 100% burn time are shown in equation 5.

$$\begin{Bmatrix} P_{\xi_{1,100}} \\ P_{\xi_{2,100}} \\ P_{\xi_{3,100}} \\ P_h \\ Q_\theta \end{Bmatrix} = \begin{bmatrix} \bar{K}_{100} \end{bmatrix} \begin{Bmatrix} \xi_{1,100} \\ \xi_{2,100} \\ \xi_{3,100} \\ h \\ \theta \end{Bmatrix} \tag{5}$$

The spring matrix, $\bar{K}_{100}$, can be obtained as the matrix product of the orthogonal 100% burn time modal mass matrix and the frequency square matrix.

$$\left[\bar{K}_{100}\right] = \begin{bmatrix} M_{1,100} & 0 & 0 & 0 & 0 \\ 0 & M_{2,100} & 0 & 0 & 0 \\ 0 & 0 & M_{3,100} & 0 & 0 \\ 0 & 0 & 0 & M_1 & 0 \\ 0 & 0 & 0 & 0 & I_{CG} \end{bmatrix} \begin{bmatrix} \omega^2{}_{1,100} & 0 & 0 & 0 & 0 \\ 0 & \omega^2{}_{2,100} & 0 & 0 & 0 \\ 0 & 0 & \omega^2{}_{3,100} & 0 & 0 \\ 0 & 0 & 0 & 0 & 0 \\ 0 & 0 & 0 & 0 & 0 \end{bmatrix} \tag{6}$$

Or numerically:

$$\left[\bar{K}_{100}\right] = \begin{bmatrix} 2.15 \times 10^5 & 0 & 0 & 0 & 0 \\ 0 & 16.9 \times 10^5 & 0 & 0 & 0 \\ 0 & 0 & 63.5 \times 10^5 & 0 & 0 \\ 0 & 0 & 0 & 0 & 0 \\ 0 & 0 & 0 & 0 & 0 \end{bmatrix} \tag{7}$$

2.5 Equations of Motion

Since the spring matrix is independent of mass, $\left[\bar{K}_{100}\right]$ is valid for any propellant loading. Thus the inertial forces (equation 3) and spring forces (equation 5) of the 0% burn time vehicle can be combined to form the equations of motion. This operation is performed below in equation 8.

$$\left[\bar{M}_0\right] \begin{Bmatrix} \ddot{\xi}_{1,100} \\ \ddot{\xi}_{2,100} \\ \ddot{\xi}_{3,100} \\ \ddot{h} \\ \ddot{\theta} \end{Bmatrix} + \left[\bar{K}_{100}\right] \begin{Bmatrix} \xi_{1,100} \\ \xi_{2,100} \\ \xi_{3,100} \\ h \\ \theta \end{Bmatrix} = 0 \tag{8}$$

2.6 Solution of Equations for Frequencies and Mode Shapes

The equations of motion (equation 8) were solved for their roots and vectors. The roots produced the frequencies at 0% burn time. The vectors formed the transformation matrix ($T_{100,0}$) relating the 100% burn time coordinates in terms of the 0% burn time coordinates (equation 9).

$$\left\{ \xi_{i,100} \right\} = \left[T_{100,0} \right] \left\{ \xi_{i,0} \right\} \tag{9}$$

The 0% burn time mode shapes $\left[T_0 \right]$ were formed in equation 10 by substitution of equation 9 into equation 1.

$$\left\{ \begin{matrix} h_i \\ \alpha_i \end{matrix} \right\} = \left[T_{100} \right] \left[T_{100,0} \right] \left\{ \xi_{i,0} \right\} = \left[T_0 \right] \left\{ \xi_{i,0} \right\} \tag{10}$$

The manipulation, $\left[T_{100} \right] \left[T_{100,0} \right]$ represents the 0% burn time transformation matrix, $\left[T_0 \right]$, which represents the 0% burn time mode shapes.

The transformation matrix at 0% burn time was normalized to put the modes in a form which is easier to plot and easier to manipulate. The first 4 modes were normalized to the gimbal and the 5th mode was normalized to 1 radian of angular deflection. The normalized transformation matrix will be designated by $\left[T_0' \right]$.

2.7 Generation of Modal Mass Matrix

The modal masses were calculated by use of the 0% burn time sectional mass matrix and the 0% burn time normalized transformation matrix. The sectional forces and sectional accelerations at 0% burn time were transformed into the modal forces and modal accelerations at 0% burn time by the operations of equation 11.

$$\begin{Bmatrix} P_{\xi_{1,0}} \\ P_{\xi_{2,0}} \\ P_{\xi_{3,0}} \\ P_{h_0} \\ Q_{\theta_0} \end{Bmatrix} = \begin{bmatrix} T_0' \end{bmatrix}^* \begin{bmatrix} M_0 \end{bmatrix} \begin{bmatrix} T_0' \end{bmatrix} \begin{Bmatrix} \ddot{\xi}_{1,0} \\ \ddot{\xi}_{2,0} \\ \ddot{\xi}_{3,0} \\ \ddot{\xi}_{1,0} \\ \ddot{\xi}_{2,0} \end{Bmatrix} \tag{11}$$

3. RESULTS

The 0% burn time modal characteristics were calculated from the 100% burn time modes. The results of these operation shall henceforth be referred to as "calculated"data.

For comparison purposes, a set of modes were calculated by the Myklestad beam vibration method for the 0% burn time vehicle. These results shall henceforth be referred to as "actual" data.

Thus, the actual and calculated results differ in that the actual data was computed directly from stiffness and inertial data; the calculated results were computed from a set of modes at 100% burn time. Any errors between actual and calculated are due only to the transformation of the 100% modes into 0% modes.

The modal deflections for the first three modes are presented in Figures 1 - 3 respectively. Frequencies for the first three body bending modes are presented in Table 1. Modal masses for the first three body bending modes are presented in Table 2.

TABLE 1

FREQUENCY COMPARISON

MODE	CALCULATED FREQUENCY (CPS)	ACTUAL FREQUENCY (CPS)	PER CENT ERROR (%E)
1st Body Bending	6.7948	6.7951	0.004
2nd Body Bending	21.261	20.946	1.50
3rd Body Bending	46.903	45.581	2.90

TABLE 2

MODAL MASS COMPARISON

MODE	CALCULATED MODAL MASS (LB SEC^2/IN)	ACTUAL MODAL MASS (LB SEC^2/IN)	PER CENT ERROR (%E)
1st Body Bending	623.72	621.48	0.36
2nd Body Bending	193.00	174.98	10.3
3rd Body Bending	499.76	197.85	152.6

4. CONCLUSIONS

The comparison of the tabulated frequency data showed a very small per cent error between the calculated and actual data. The percent error in the first, second, and third mode were .004%, 1.50%, and 2.90% respectively.

The comparison of the mode shapes showed that the deviation in mode shape got progressively worse. The first mode in Figure 1 exhibits no plottable errors. The second mode as shown in Figure 2 has a small deviation but is a relatively accurate mode. The third mode as shown in Figure 3 has a large deviation between the actual and calculated data. The method of solution would have been exact if an infinite number of modes were used. Since a finite number of modes were used, the higher modes suffered.

The modal masses are a function of sectional masses and mode shapes. The error in the mode shape shows up as a squared term in the modal mass computations. The rapid deterioration in modal masses for the higher modes is evident from the comparison of calculated and actual results of Table 2. The first modal mass is very close (.36%), the second is a fair approximation (10.3%), and the third modal mass (152.6%) is out of the range of usefulness. Therefore, the results of the third mode must be discarded.

In conclusion, the method outlined herein is adequate for generating the first two body bending modes of the Dynamics Vehicle given a set of three empty vehicle modes. Therefore, only the empty vehicle modes need be measured if no more than two resulting modes are desired.

FREE-FREE BODY BENDING DEFLECTIONS
SATURN S-IVB/IB AT 0% BURN TIME
NORMALIZED TO GIMBAL POINT AT STATION 100
ENGINE MASS AND SLOSHING MASSES REMOVED

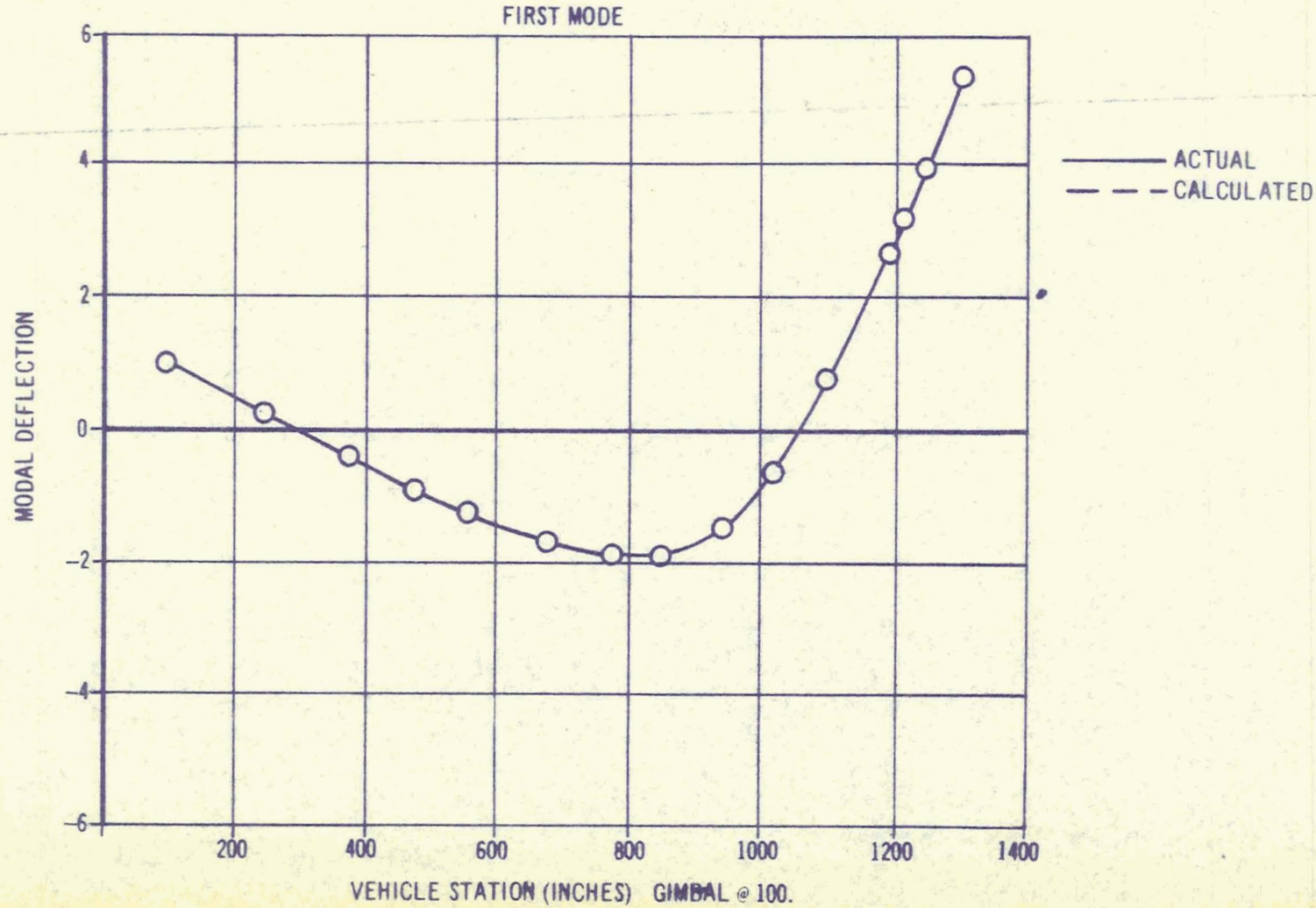

FIGURE 1

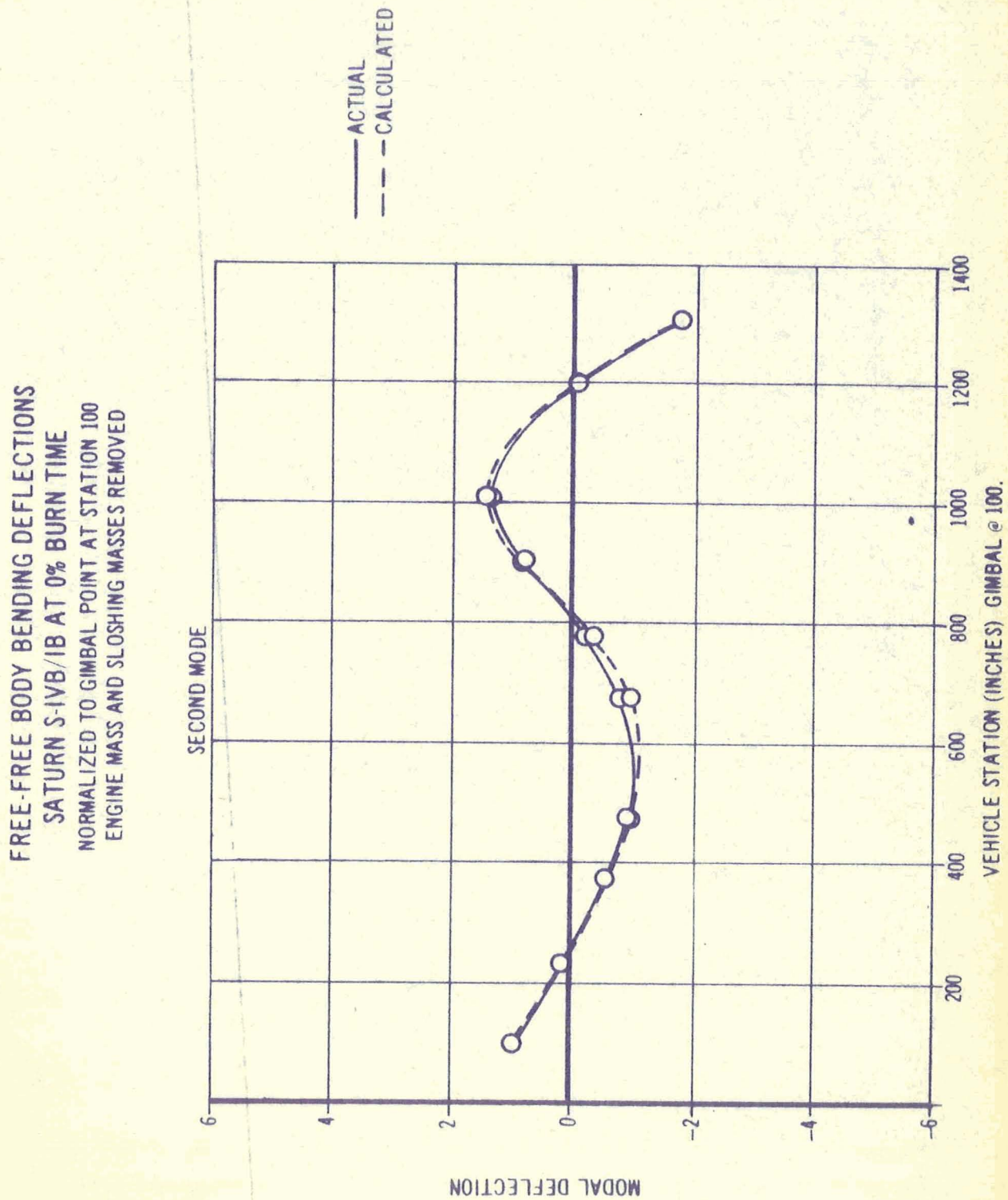
FREE-FREE BODY BENDING DEFLECTIONS
SATURN S-IVB/IB AT 0% BURN TIME
NORMALIZED TO GIMBAL POINT AT STATION 100
ENGINE MASS AND SLOSHING MASSES REMOVED
SECOND MODE
ACTUAL
CALCULATED
MODAL DEFLECTION
6
4
2
0
-2
-4
-6
200
400
600
800
1000
1200
1400
VEHICLE STATION (INCHES) GIMBAL @ 100.

FIGURE 2

FREE-FREE BODY BENDING DEFLECTIONS
SATURN S-IVB/IB AT 0% BURN TIME
NORMALIZED TO GIMBAL POINT AT STATION 100
ENGINE MASS AND SLOSHING MASSES REMOVED

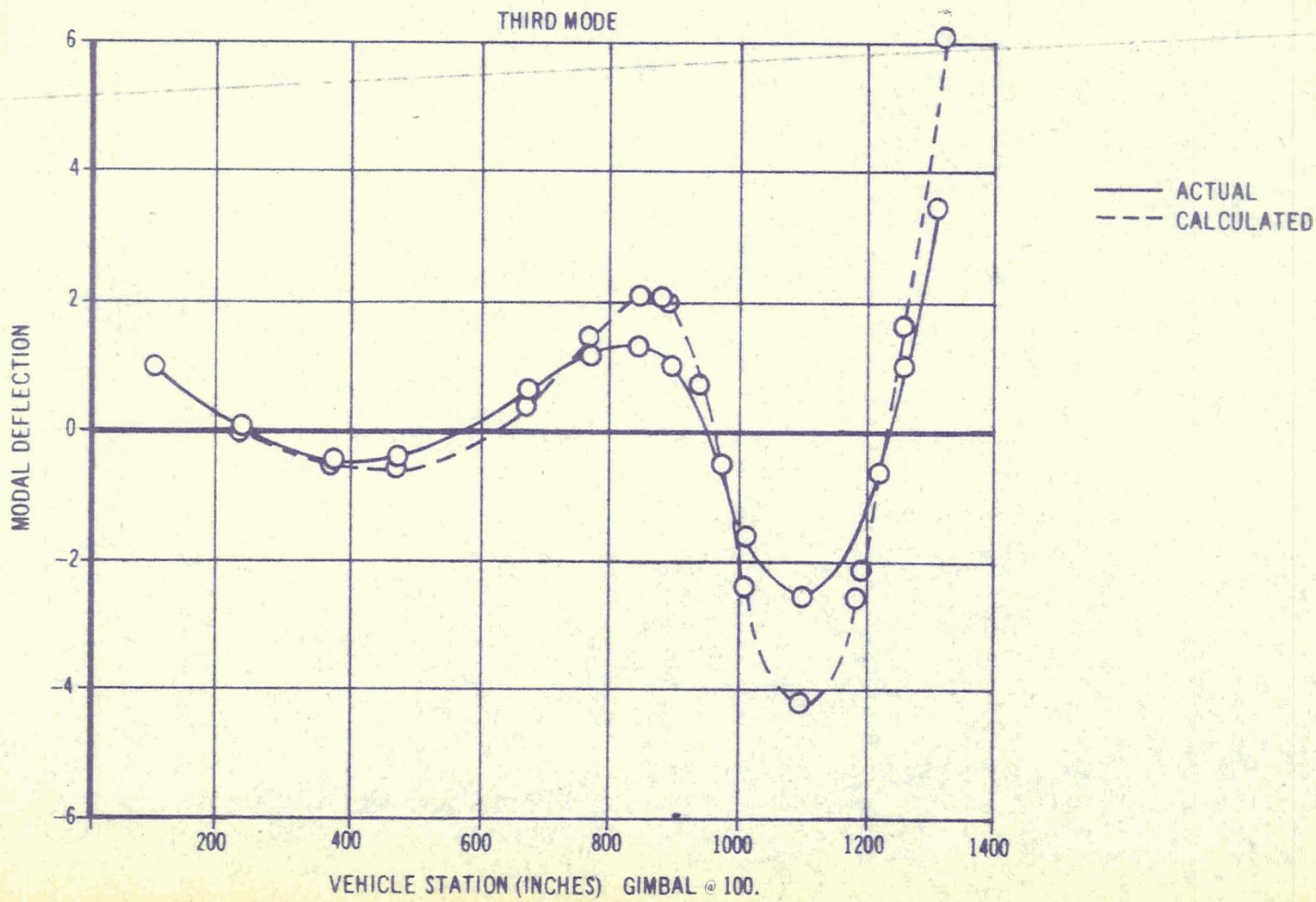

FIGURE 3

APPENDIX A

BASIC DATA

A-1 Transformation Matrix Relating Sectional Deflections in Terms of 100% Burn Time Coordinates

$$\begin{Bmatrix} h_1 \\ \alpha_1 \\ \vdots \\ h_{32} \\ \alpha_{32} \end{Bmatrix} = \begin{bmatrix} T_{100} \end{bmatrix} \begin{Bmatrix} \xi_{1,100} \\ \xi_{2,100} \\ \xi_{3,100} \\ h \\ \theta \end{Bmatrix}$$

T_{100}:

Sect. No.	Column 1	Column 2	Column 3	Column 4	Column 5
1	+.129000 +1	+.152549 +1	+.170259 +1	+.100000 +1	
2	-.289990 -2	-.525500 -2	-.702650 -2	+.100000 +1	
3	+.100000 +1	+.100000 +1	+.100000 +1	+.100000 +1	+.100000 +3
4	-.289990 -2	-.525500 -2	-.702650 -2	+.100000 +1	
5	+.942000 0	+.894959 0	+.859700 0	+.100000 +1	+.120000 +3
6	-.289969 -2	-.524889 -2	-.700269 -2	+.100000 +1	
7	+.884129 0	+.792150 0	+.726759 0	+.100000 +1	+.140000 +3
8	-.288570 -2	-.500110 -2	-.620209 -2	+.100000 +1	
9	+.840889 0	+.717969 0	+.636330 0	+.100000 +1	+.155000 +3
10	-.287849 -2	-.488169 -2	-.583370 -2	+.100000 +1	
11	+.794870 0	+.640410 0	+.544639 0	+.100000 +1	+.171000 +3
12	-.287349 -2	-.480360 -2	-.560019 -2	+.100000 +1	
13	+.760400 0	+.582919 0	+.477879 0	+.100000 +1	+.183000 +3
14	-.287169 -2	-.477599 -2	-.552139 -2	+.100000 +1	
15	+.740299 0	+.549530 0	+.439330 0	+.100000 +1	+.190000 +3
16	-.287089 -2	-.476540 -2	-.549190 -2	+.100000 +1	
17	+.611309 0	+.337830 0	+.199719 0	+.100000 +1	+.235000 +3
18	-.286089 -2	-.462629 -2	-.511330 -2	+.100000 +1	
19	+.568400 0	+.268590 0	+.123419 0	+.100000 +1	+.250000 +3
20	-.285940 -2	-.460570 -2	-.505780 -2	+.100000 +1	

Sect. No.	Column 1	Column 2	Column 3	Column 4	Column 5
21	+.476990 0	+.122400 0	-.352030 -1	+.100000 +1	+.282000 +3
22	-.285360 -2	-.452700 -2	-.484629 -2	+.100000 +1	
23	+.213349 0	-.278969 0	-.440019 0	+.100000 +1	+.375000 +3
24	-.280980 -2	-.404919 -2	-.375620 -2	+.100000 +1	
25	-.634809 -1	-.643540 0	-.732250 0	+.100000 +1	+.475000 +3
26	-.271919 -2	-.318910 -2	-.201990 -2	+.100000 +1	
27	-.274379 0	-.862009 0	-.831290 0	+.100000 +1	+.554000 +3
28	-.261509 -2	-.232000 -2	-.483059 -3	+.100000 +1	
29	-.565049 0	-.914700 0	-.531790 0	+.100000 +1	+.677000 +3
30	-.208740 -2	+.143269 -2	+.495639 -2	+.100000 +1	
31	-.599830 0	-.886209 0	-.443000 0	+.100000 +1	+.694000 +3
32	-.200389 -2	+.191610 -2	+.547690 -2	+.100000 +1	
33	-.635089 0	-.847290 0	-.340099 0	+.100000 +1	+.712000 +3
34	-.191320 -2	+.240330 -2	+.594059 -2	+.100000 +1	
35	-.743469 0	-.640150 0	+.721500 -1	+.100000 +1	+.775000 +3
36	-.152339 -2	+.408200 -2	+.689320 -2	+.100000 +1	
37	-.828110 0	-.249780 0	+.559219 0	+.100000 +1	+.850000 +3
38	-.726330 -3	+.609679 -2	+.552269 -2	+.100000 +1	
39	-.839469 0	-.247360 -1	+.689389 0	+.100000 +1	+.884000 +3
40	+.611509 -4	+.703830 -2	+.190040 -2	+.100000 +1	
41	-.833750 0	+.841019 -1	+.690700 0	+.100000 +1	+.899000 +3
42	+.702110 -3	+.743709 -2	-.180769 -2	+.100000 +1	
43	-.763860 0	+.403910 0	+.417759 0	+.100000 +1	+.941000 +3
44	+.259370 -2	+.750250 -2	-.103299 -1	+.100000 +1	
45	-.662639 0	+.621889 0	+.421269 -1	+.100000 +1	+.972000 +3
46	+.391769 -2	+.639849 -2	-.134080 -1	+.100000 +1	
47	-.458910 0	+.825480 0	-.528730 0	+.100000 +1	+.101400 +4
48	+.574429 -2	+.296750 -2	-.127440 -1	+.100000 +1	
49	+.988469 -1	+.819820 0	-.122019 +1	+.100000 +1	+.109599 +4
50	+.771459 -2	-.309940 -2	-.284410 -2	+.100000 +1	
51	+.847730 0	+.265690 0	-.772440 0	+.100000 +1	+.118400 +4
52	+.910429 -2	-.891769 -2	+.124070 -1	+.100000 +1	
53	+.902599 0	+.210990 0	-.694240 0	+.100000 +1	+.119000 +4
54	+.918450 -2	-.931129 -2	+.136490 -1	+.100000 +1	
55	+.116299 +1	-.667339 -1	-.255149 0	+.100000 +1	+.121799 +4

Sect. No.	Column 1	Column 2	Column 3	Column 4	Column 5
56	+.939580 -2	-.104379 -1	+.175089 -1	+.100000 +1	
57	+.142830 +1	-.372690 0	+.288440 0	+.100000 +1	+.124599 +4
58	+.953089 -2	-.113000 -1	+.209389 -1	+.100000 +1	
59	+.150480 +1	-.464410 0	+.461620 0	+.100000 +1	+.125400 +4
60	+.957509 -2	-.116150 -1	+.222929 -1	+.100000 +1	
61	+.201759 +1	-.112230 +1	+.184179 +1	+.100000 +1	+.130700 +4
62	+.969459 -2	-.125519 -1	+.267879 -1	+.100000 +1	
63	+.202730 +1	-.113490 +1	+.186860 +1	+.100000 +1	+.130799 +4
64	+.969469 -2	-.125519 -1	+.267900 -1	+.100000 +1	

A-2 Sectional Mass Matrix Relating The Sectional Masses At 0% Burn Time Coordinates.

$$\begin{Bmatrix} P_1 \\ Q_1 \\ \vdots \\ P_{32} \\ Q_{32} \end{Bmatrix} = \begin{bmatrix} & M_0 & \end{bmatrix} \begin{Bmatrix} \ddot{h}_1 \\ \ddot{\alpha}_1 \\ \vdots \\ \ddot{h}_{32} \\ \ddot{\alpha}_{32} \end{Bmatrix}$$

$\underline{M_0}$:

Sect. No.	Column 1	Column 2
3	+.111360 0	+.556790 0
4	+.556790 0	+.143330 +4
5	+.855179 0	-.661480 +1
6	-.661480 +1	+.721839 +2
7	+.240459 0	-.137290 0
8	-.137290 0	+.610440 +1
9	+.251200 +1	+.119530 +2
10	+.119530 +2	+.767879 +2
11	+.148259 +2	+.101780 +1
12	+.101780 +1	+.225299 +3
13	+.194919 +2	-.717540 +2
14	-.717540 +2	+.189150 +4
15	+.506580 +2	+.314410 +3
16	+.314410 +3	+.333230 +4
17	+.770110 +2	-.473169 +2
18	-.473169 +2	+.183950 +4
19	+.116480 +3	+.552019 +3
20	+.552019 +3	+.970639 +4
21	+.162419 +3	+.306190 +3
22	+.306190 +3	+.528019 +5
23	+.384410 +2	+.870469 +2
24	+.870469 +2	+.294820 +5

Sect. No.	Column 1		Column 2	
25	+.186139	+2	-.168500	+3
26	-.168500	+3	+.212179	+5
27	+.361299	+2	+.353019	+3
28	+.353019	+3	+.386929	+5
29	+.575450	+1	-.860259	+2
30	-.860259	+2	+.341379	+4
31	+.348969	+1	+.872419	0
32	+.872419	0	+.892769	+2
33	+.302429	+1	+.108940	+2
34	+.108940	+2	+.442660	+3
35	+.216530	+1	+.232559	+1
36	+.232560	+1	+.853559	+3
37	+.119759	+1	-.143309	+2
38	-.143309	+2	+.464389	+3
39	+.390950	0	-.204379	+1
40	-.204370	+1	+.301500	+2
41	+.332629	+2	-.194870	+3
42	-.194870	+3	+.122589	+4
43	+.472629	0	-.129969	+1
44	-.129969	+1	+.560459	+2
45	+.472629	0	+.129969	+1
46	+.129969	+1	+.560459	+2
47	+.151759	+2	-.657150	+2
48	-.657150	+2	+.626280	+4
49	+.646660	+1	-.438839	+2
50	-.438839	+2	+.458669	+4
51	+.267780	+1	-.548950	+2
52	-.548950	+2	+.161830	+4
53	+.968559	0	+.532709	+1
54	+.532709	+1	+.526250	+2
55	+.729269	+1	+.854610	+1
56	+.854610	+1	+.413780	+3
57	+.512769	+1	-.256379	+2
58	-.256379	+2	+.266639	+3

Sect. No.	Column 1	Column 2
59	+.502870 +1	+.413469 +2
60	+.413469 +2	+.737219 +3
61	+.196330 +1	-.291879 +2
62	-.291879 +2	+.546360 +3
63	+.209969 -1	-.527269 -2
64	-.527269 -2	+.176150 -2